Available online at www.sciencedirect.com
SCIENCE DIRECT®
Journal of Sound and Vibration 266 (2003) 785–804
JOURNAL OF SOUND AND VIBRATION
www.elsevier.com/locate/jsvi

A numerical study on the flow and sound fields of centrifugal impeller located near a wedge

Wan-Ho Jeon[a,*], Duck-Joo Lee[b]

[a] *DA Research Lab, LG Electronics Inc, 327-23, Kasan-dong, Kumchon-gu, Seoul 153-802, South Korea*
[b] *Department of Aerospace Engineering, KAIST, Yusong-gu, Taejon 305 701, South Korea*

Received 11 March 2002; accepted 23 September 2002

Abstract

Centrifugal fans are widely used and the noise generated by these machines causes one of the serious problems. In general, the centrifugal fan noise is often dominated by tones at blade passage frequency and its higher harmonics. This is a consequence of the strong interaction between the flow discharged from the impeller and the cut-off in the casing. However, only a few researches have been carried out on predicting the noise because of the difficulty in obtaining detailed information about the flow field and considering the scattering effect of the casing. The objective of this study is to understand the generation mechanism of sound and to develop a prediction method for the unsteady flow field and the acoustic pressure field of the centrifugal impeller. A discrete vortex method is used to model the centrifugal impeller and a wedge and to calculate the flow field. The force of each element on the blade is calculated by the unsteady Bernoulli equation. Lowson's method is used to predict the acoustic source. In order to consider the scattering and diffraction effects of the casing, Kirchhoff–Helmholtz boundary element method (BEM) is developed. The source of Kirchhoff–Helmholtz BEM is newly developed, so the sound field of the centrifugal fan can be obtained. A centrifugal impeller and wedge are used in the numerical calculation and the results are compared with the experimental data. Reasonable results are obtained not only for the peak frequencies but also for the amplitudes of the tonal sound. The radiated acoustic field shows the diffraction and scattering effect of the wedge.

1. Introduction

Centrifugal turbomachines are common devices used in many flow control applications due to their ability to achieve relatively high-pressure ratios in a short axial distance compared with axial

*Corresponding author.
E-mail address: whjeon@lge.com (W.-H. Jeon).

0022-460X/03/$ - see front matter © 2002 Elsevier Ltd. All rights reserved.
doi:10.1016/S0022-460X(02)01357-3

fans. They are often found in gas turbine engines, heating ventilation and air-conditioning systems and pumps. Because of their widespread use, the noise generated by these machines causes one of the serious problems. The noise is often dominated by tones at the blade passage frequency and its higher harmonics. This is a consequence of the strong interactions between the flow discharged from the impeller and the cut-off in the casing [1]. In addition to the discrete tones, the broadband noise is generated from the trailing edge due to the fluctuations of the turbulent boundary layers or separated flows on the impeller blade.

In the past, noise reduction method and the numerical method to predict the flow and acoustic fields of an axial fan have been studied by many researchers. On the contrary, the numerical prediction method for the centrifugal fan has not been reported, yet. It is because of the scattering effect of the casing. In order to calculate the radiated acoustic field of a centrifugal fan, the modification of the generated noise by the casing should be considered. Relatively, noise reduction methods of the tonal noise of the centrifugal fan are well studied. Neise [2] summarized the efforts in reducing the blade passage tone by changing the geometry of the impeller and the cut-off. Other efforts such as sloped cut-off and impeller blades by Embleton have been utilized [3]. Neise and Koopmann [4] used a resonator to reduce the blade passage tones by canceling the unsteady aerodynamic noise sources at the cut-off. However, many aspects of sound generation by the unsteady flow in turbomachinery are still poorly understood. So the focus of this study is on the understanding and predicting of the aerodynamic noise generated by the centrifugal turbomachinery.

In order to understand the aeroacoustic source of a centrifugal fan, we need detailed information of the flow field. Therefore, the numerical method to analyze the flow field of the centrifugal fan is necessary. For the flow field with moving boundaries such as impeller, Lagrangian methods are preferable because of the grid-free characteristics. However, while moving boundaries are easily tackled, the implement of the no-slip condition on the blade is difficult. In the Lagrangian methods, this no-slip condition is satisfied by a vorticity generation process all along the solid boundaries, which requires a large number of vortex particles with the no-slip condition. So, under the hypothesis of the inviscid fluid, a vortex particle is shed at the trailing edge of a blade. This inviscid Lagrangian method has been used in unsteady airfoil theory and studied for fan flow analysis [5–7]. Kiya studied the separated flow field of a centrifugal impeller by the discrete vortex method (DVM) [8]. A centrifugal fan in the casing is analyzed by Evangelos et al. [5] by the Lagrangian method.

The characteristics of aerodynamic sound have been studied using acoustic similarity law through numerical and experimental methods [9–12]. The basic concept of the acoustic similarity law is that the radiated sound can be expressed as a non-dimensional product of the Reynolds number (Re) raised to an exponent β, the Mach number (Ma) raised to an exponent α, a spectral distribution function, $F(ST)$, and an acoustic frequency response function, $G(He)$. Here the $F(ST)$ function is related to the aerodynamic sound with Re and Ma. Based on this similarity law, Chanaud concluded that in general the dipole is dominant for the centrifugal impeller sound [9]. Neise [12] shows that the primary causes of fan noise are the fluctuating forces of the blades. In order to obtain acoustic signal from the unsteady force fluctuation of the blades, we use Lowson's equation in Ref. [13]. Lowson derived the formula for predicting the acoustic field generated by the moving point force from the wave equation. By applying this equation to each blade element, we can predict the acoustic pressure generated by the impeller. But Lowson's equation is applied

only in the free field. The effects of the solid boundaries cannot be considered in this method. The scattering effect of acoustic is easily calculated by the boundary element method (BEM). So the Kirchhoff–Helmholtz BEM is newly developed to calculate the solid boundary to take into account the scattering effect of the solid boundaries such as casing and duct.

This paper is organized in the following manner. The numerical method is described in Section 2. The vortex method is used to calculate the flow field and Lowson's method is used to predict the acoustic source, which is used for the scattered acoustic field in BEM. In order to validate the proposed method, results are given in Section 3 of the present paper for the centrifugal fan experimentally tested by Weidemann [1]. The results of the flow fields and the acoustic signature are given in Section 3. Conclusions are presented in Section 4.

2. Numerical method

2.1. Freefield acoustic calculation

Neise shows that the dipole, especially the unsteady force fluctuation, is the dominant source of the fan noise [12]. The most prominent source of the dipole in the centrifugal fan is the rotating impeller. Therefore, the sound field generated by the forces of the impeller blades is considered in this paper.

A general formula for the sound field of a point force in an arbitrary motion is derived by Lowson in 1965 as below [13]:

$$\rho - \rho_0 = \left[\frac{x_i - y_i}{4\pi a_0^3 r^2 (1 - M_r)^2} \left\{ \frac{\partial F_i}{\partial t} + \frac{F_i}{1 - M_r} \frac{\partial M_r}{\partial t} \right\} \right], \tag{1}$$

where

$$M_r = \frac{M_i r_i}{r}. \tag{2}$$

F_i is the calculated force of the impeller blade and a_0 is the speed of sound. x_i and y_i are the source position and absorber position and r is the distance between them.

Eq. (1) refers to the effect of an isolated point force. In order to apply the equation to an impeller blade, the distributed loading over the impeller blade is divided by small point elements, as is common in propeller noise theory.

We must consider whether the aeroacoustic sources are acoustically compact or not. For the impeller, the transition from compact to non-compact radiation will occur when the blade leading and trailing edges are no longer located within an acoustic wavelength. At frequencies above this criterion, the acoustic noise is generated by a set of independent acoustic sources distributed across the blade surface. So, if the mesh of the blade is sufficiently fine, a compact acoustic source can be considered with this method.

The force on the blade is represented by a point force, which acts on that element. By applying Eq. (1) to each blade element, we can predict the acoustic pressure in the free field. But, the effects of the scattering and diffraction due to the solid body cannot be considered. Only the behavior of

the noise source and its radiation to the free field can be estimated. And this acoustic pressure is used an acoustic source in BEM, which will be described in detail later.

2.2. Flow calculation

To simulate the noise generation, only an impeller and a wedge are chosen without the casing as shown in Fig. 1. This is experimentally tested by Weidemann [1]. The unsteady flow is generated due to the rotation of the impeller at an angular velocity Ω near a wedge. For the centrifugal fan, the rotation of the impeller results in an inflow across the inlet section. Let $Q(t)$ denote the flow rate, represented by a source located at the center of the impeller. Assuming the fluid is incompressible and inviscid, the main feature of the flow considered is the non-zero circulation around every impeller blade.

We assume that the impeller rotates with a constant angular velocity and the flow field of the impeller is incompressible and inviscid. The impeller has NB number of blades and each blade has nc number of elements. Bound vortices are located at the 1/4 point of each element and control points are taken at the 3/4 point. Wake vortices are shed from the trailing edge of the impeller at every time step to satisfy the Kutta condition. Shed vortices are convected with the local induced velocity. The inlet flow is modelled by a point source located at the center of the impeller. The wedge is modelled with source panels where the control point is taken at the center of the element.

The induced velocity at a point of the body ($\vec{x}_c$) is shown as below:

$$\vec{U}(\vec{x}_c; t) = \vec{U}_Q(\vec{x}_c; t) + \vec{U}_{bv}(\vec{x}_c; t) + \vec{U}_{wv}(\vec{x}_c; t) + \vec{U}_{sp}(\vec{x}_c; t). \tag{3}$$

The first term of the right-hand side represents the velocity at $\vec{x}_c$ induced by the point source and the second term represents the velocity induced by bound vortices of the impeller. The third term represents the velocity induced by wake vortices and the fourth term represents the velocity induced by source panels.

The unknown strengths of the bound vortices and the source panels are calculated with the normal boundary condition that there is no flow across the surface boundary (Eq. (4)) and

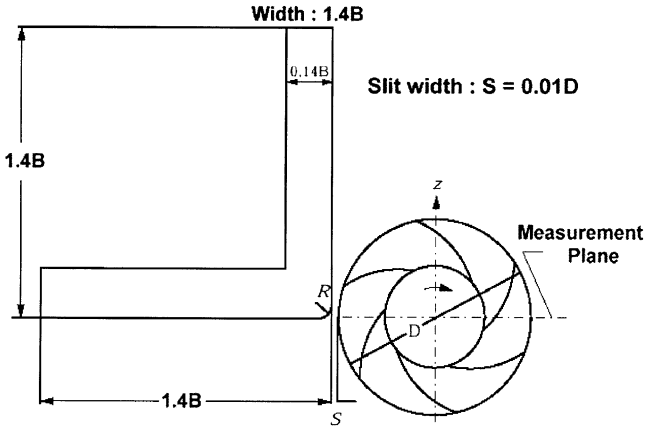

Fig. 1. Dimensions of the impeller and wedge used by Weidemann.

Kelvin's theorem (Eq. (5))[7,8]:

$$\left[\vec{U}_Q(\vec{x}_c;t)_j+\vec{U}_{bv}(\vec{x}_c;t)_j+\vec{U}_{wv}(\vec{x}_c;t)_j+\vec{U}_{sp}(\vec{x}_c;t)_j\right]\bullet\vec{n}(\vec{x}_c)j = \begin{cases}\Omega((\vec{n}(\vec{x}_{cj})\times\vec{x}_{cj}(t)) & \text{impeller},\\ 0 & \text{wedge},\end{cases} \tag{4}$$

$$\frac{\mathrm{D}\Gamma_m(t)}{\mathrm{D}t}=0,$$
$$\left[\sum_{k=1}^{nc}\Gamma_{bk}(t)+\sum_{k=1}^{nv}\Gamma_{wk}(t)\right]_m=0. \tag{5}$$

Here, Γ_m is the total circulation of that blade, composed of the bound vortices (Γ_b) of the impeller and shed wake vortices (Γ_w) and Ω means the rotating angular velocity. The positive value indicates that the direction of the rotation is the clockwise rotation. The subscripts m, nc, and nv mean the number of blade, the number of elements at one blade and the number of shed wake vortex particles.

In order to calculate the acoustic pressure from the flowfield data, the force of each blade must be calculated. The force of each element on the blade is calculated by the unsteady Bernoulli equation:

$$\vec{F}_{nj}=\rho\left\{\vec{U}(\vec{x}_c)\bullet\vec{\tau}_j\frac{\Gamma_{bj}}{\Delta s_j}+\frac{\partial}{\partial t}\sum_{k=1}^{j}\Gamma_{bk}\right\}\Delta s_j. \tag{6}$$

Here, $\vec{F}$, $\vec{\tau}$ and Δs_j are the normal force, tangential vector and the length of that element. ρ and U are the density and the local induced velocity.

2.3. Acoustic field calculation

In the case of the centrifugal impeller and wedge, experiment results contain the effect of acoustic characteristics of the wedge such as reflection, scattering and diffraction of the wedge. These effects are schematically viewed in Fig. 2. In the figure we can see that the sound will propagate with some directivity angle—the sound will radiate dominantly at 135° and 315° from the measurement plane. But there is no method to consider this scattering effect with centrifugal impeller source. So we derive a Kirchhoff–Helmholtz BEM to calculate the scattering effect of the wedge with a known centrifugal impeller source.

The disadvantage of the BEM is that the source is difficult to model. Moving monopole, dipole and normal velocity vibration are possible sources in BEM. So, the centrifugal fan is difficult to solve by BEM. We need the new method to consider the complex acoustic source, or aeroacoustic source in BEM and the method proposed by this paper could be one of them. This method—Kirchhoff–Helmholtz BEM—could be derived by considering some source mesh in a computational domain. This mesh surrounds the source region—in this case, the impeller. The acoustic value of this Kirchhoff source mesh can be calculated by Lowson's equation, and considered as a source in BEM.

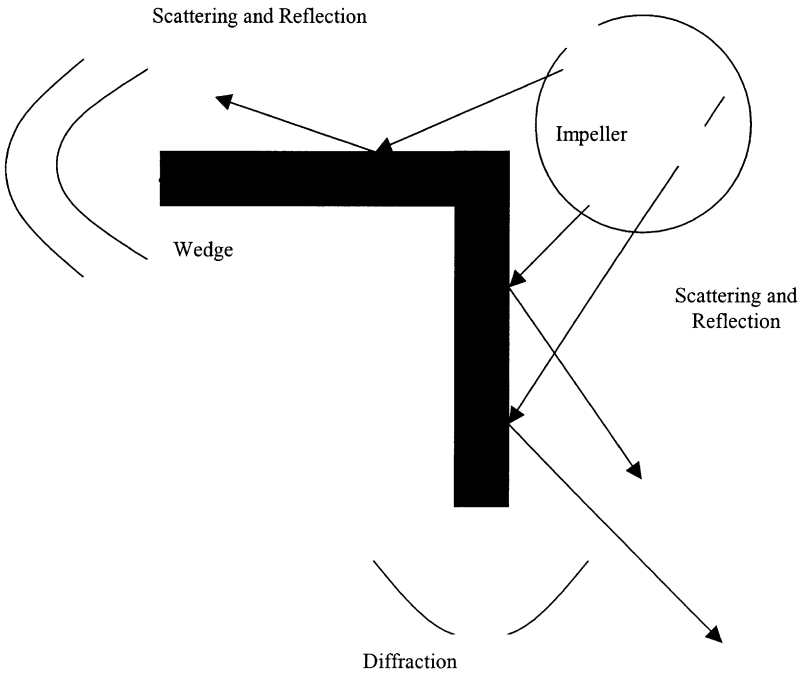

Fig. 2. Acoustic field due to wedge.

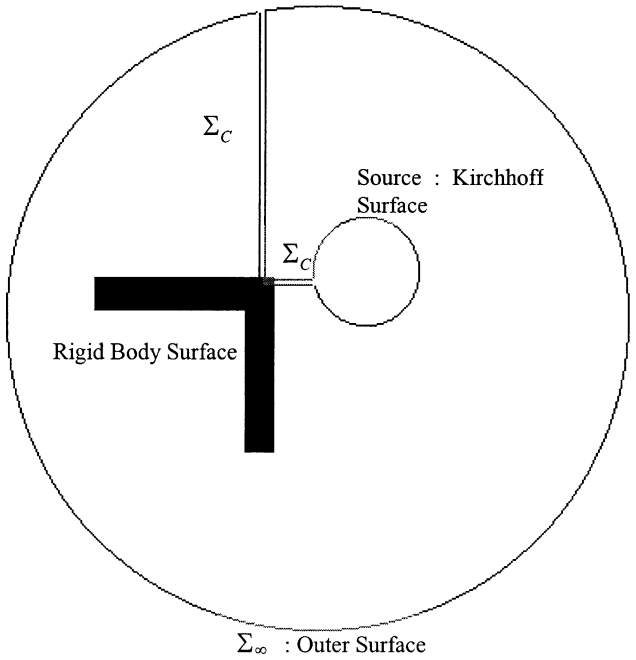

Fig. 3. Integral contours for exterior/interior acoustic field problem.

This section gives a brief description of the boundary integral formulation used in the present study. Consider a scattering object bounded by a closed surface S as shown in Fig. 3. Let s denote the Kirchhoff surface that surrounds the source region—impeller, jet and wake, etc. Then, the most general solution of acoustic problem for harmonic sources is the Helmholtz integral equation, which represents the sound pressure at any point in terms of the surface pressure and its normal velocity:

$$C(P)\,\phi(P) = \int_S \left[\phi(Q)\frac{\partial G}{\partial n}(P,Q) - \frac{\partial \phi}{\partial n}\,G(P,Q)\right] \mathrm{d}S(Q). \tag{7}$$

Here, ϕ is the velocity potential, $C(x)$ is the solid angle at the field point x and $n(x)$ is the surface normal unit vector from the interior of the body. $G(P,Q)$ is the free space Green function

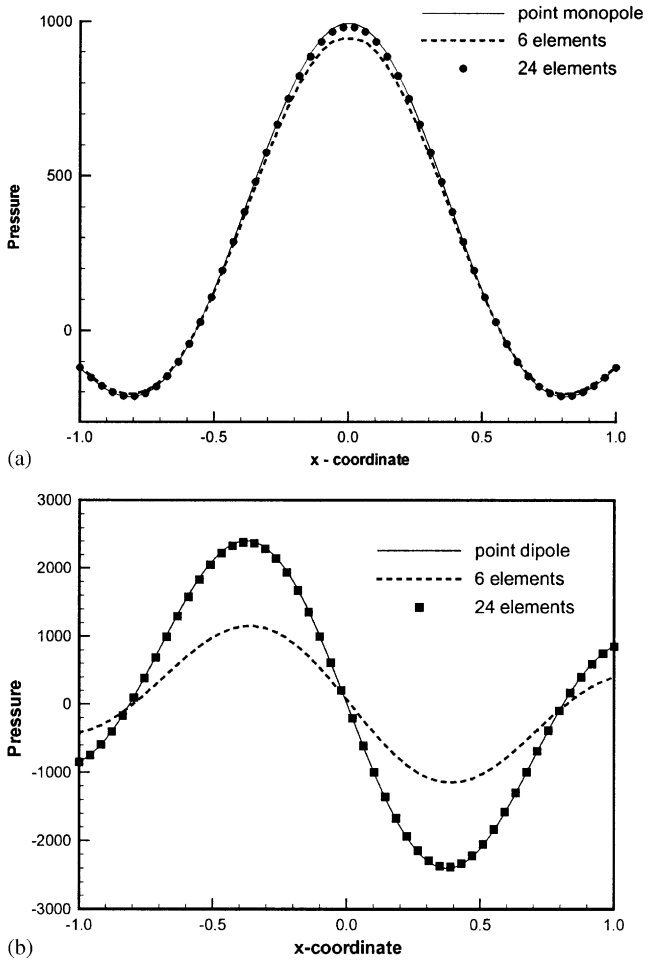

Fig. 4. Comparison of the Kirchhoff source with the point monopole and dipole. (a) Pressure distribution with respect to x co-ordinate at free field. Kirchhoff surface with 24 elements is exact with the point monopole source. (b) Pressure distribution with respect to x co-ordinate at free field. Kirchhoff surface with 24 elements is exact with the point dipole source at 300 Hz.

satisfying the inhomogeneous Helmholtz equation in three dimensions:

$$G(r) = \frac{e^{-jkr}}{4\pi r}, \tag{8}$$

where r is the distance between the "receiver" and "source" and κ is the wave number.

In the case of the Kirchhoff–Helmholtz BEM, due to the surface integral of Kirchhoff surface, Kirchhoff surface integral term is added in Eq. (10):

$$C(P)\phi(P) = \int_S \left[\phi(Q)\frac{\partial G}{\partial n}(P,Q) - \frac{\partial \phi}{\partial n}G(P,Q)\right] dS(Q) + \int_{\text{Kirchhoff}} \left[\phi(K)\frac{\partial G}{\partial n}(P,K) - \frac{\partial \phi}{\partial n}G(P,K)\right] ds(K). \tag{9}$$

Here, index K means the value of the Kirchhoff mesh. The value of this Kirchhoff source term is calculated from Eq. (1) at the Kirchhoff surface points.

The non-uniqueness problem, occuring at certain frequencies equal to the eigenwavenumber of the corresponding interior domain, is overcome by Shenck's proposal [14], which adds some constraints, the number of which is equivalent to that of augmented points in constructing the matrix equation. The positions of augmented points are selected randomly to maximize the possibility that at least one augmented point can deviate from the interior eigenmodal surfaces, which gives the good results as described by Seybert et al. [15]. An arbitrary number of four

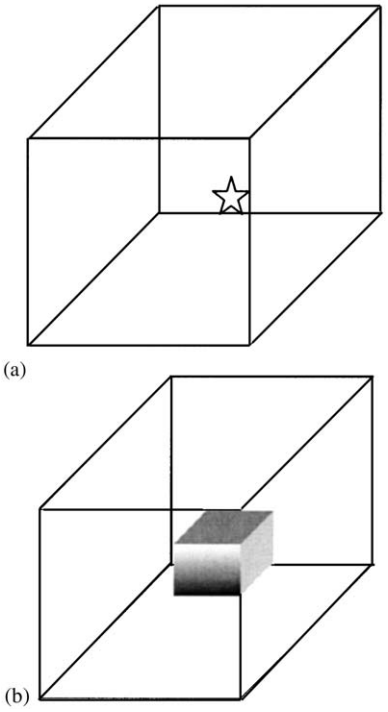

Fig. 5. Source and its Kirchhoff surface within a rectangular box. (a) Monopole source in a rectangular box. (b) Kirchhoff source in a rectangular box.

augmented points was given to each body in our calculations. As the frequency increases, however, an additional number of the augmented points is required to settle the non-uniqueness problem.

2.4. Acoustic similarity law

Sound measurements concerned with similarity over a wide range of impeller sizes were made by Weidemann [1]. The general relationship among non-dimensional parameters developed by Weidemann may be written as follows:

$$\Delta\tilde{p}/P_0 = Ma^{\alpha}\, Re^{\beta}\, F(St)\, G(He). \tag{10}$$

Here $\Delta\tilde{p}$, Ma and Re mean the r.m.s. value of the sound pressure, the Mach number of the flow and the Reynolds number.

The first two terms in Eq. (10) govern the influence of tip speed and impeller diameter as well as the influence of viscosity. The function $F(St)$ describes the spectral distribution of the sound

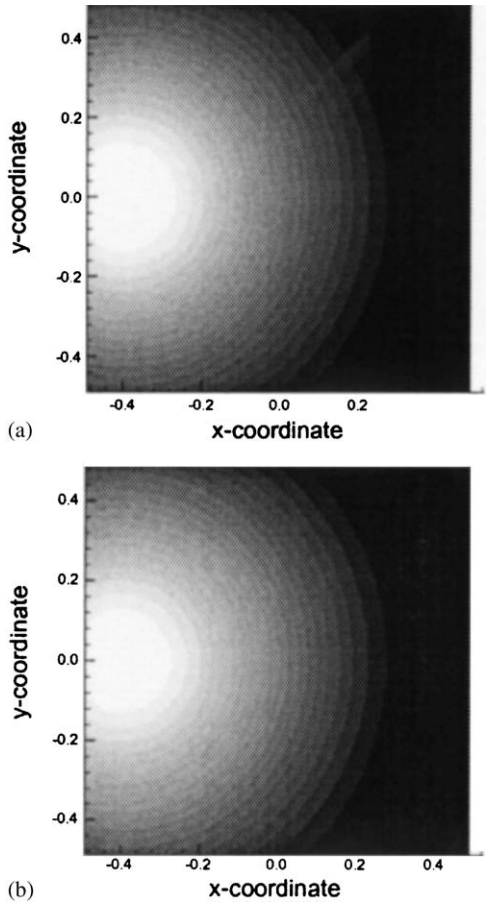

Fig. 6. Comparison of the Kirchhoff–Helmhplyz BEM on the box with the point monopole (24 elements, 300 Hz). (a) Sound pressure by the point monopole source at $x = -0.4$. (b) Sound pressure by Kirchhoff surface at $x = -0.4$.

source generated. Eq. (10) implies that the dependence on Mach number and Reynolds number is the same for all Strouhal numbers, St. The first three terms determine the generation of sound, since all of them depend on the rotor velocity. But $G(He)$ is a function of a purely geometric parameter. He is the Helmholtz number, frequency divided by acoustic speed, which is not related

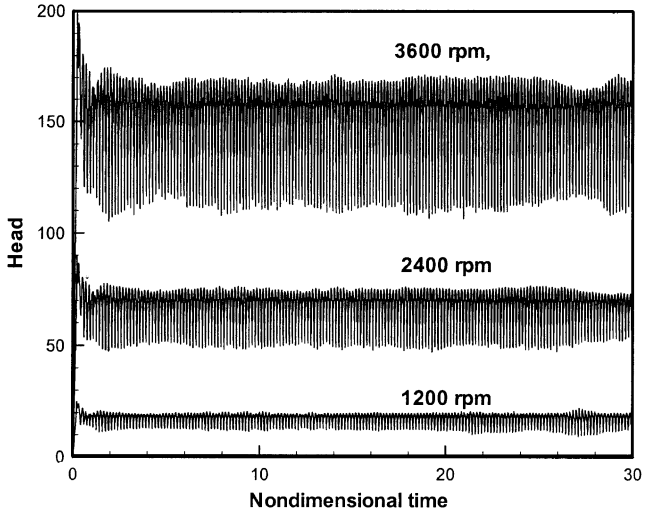

Fig. 7. Variations of head with time at various r.p.m.

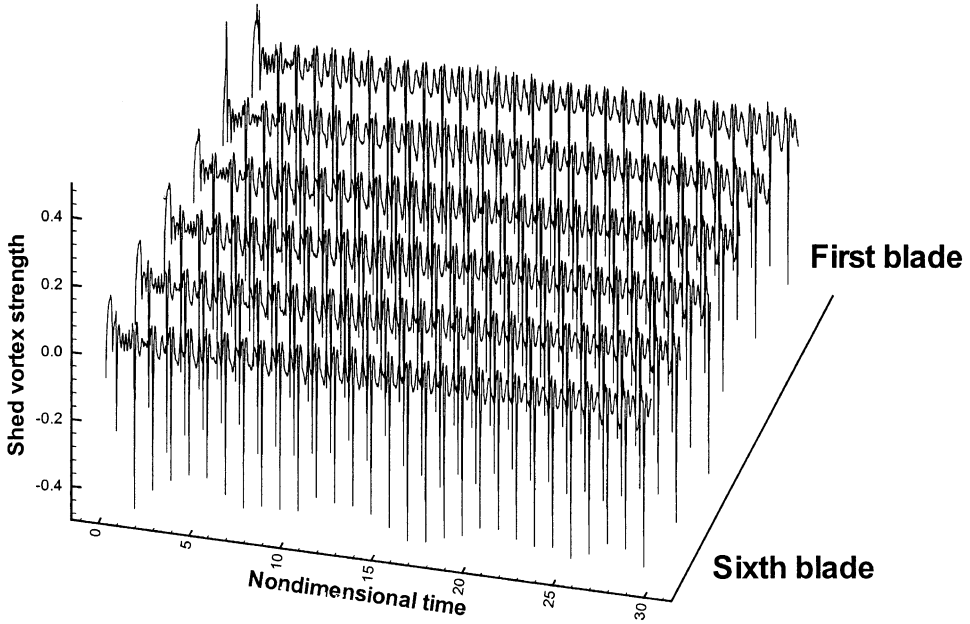

Fig. 8. Variations of the shed vortex strength with time at each blade.

to the impeller velocity. Therefore, $G(He)$ can be considered as an acoustic frequency response function which describes the sound radiation characteristics of the fan.

Values 2.6 and 0.2 were found for the influence of Mach number (α) and Reynolds number (β) on the discrete frequency sound. In this numerical method, the exponent of the Mach number and $F(St)$ can be predicted, which is related to the sound generation.

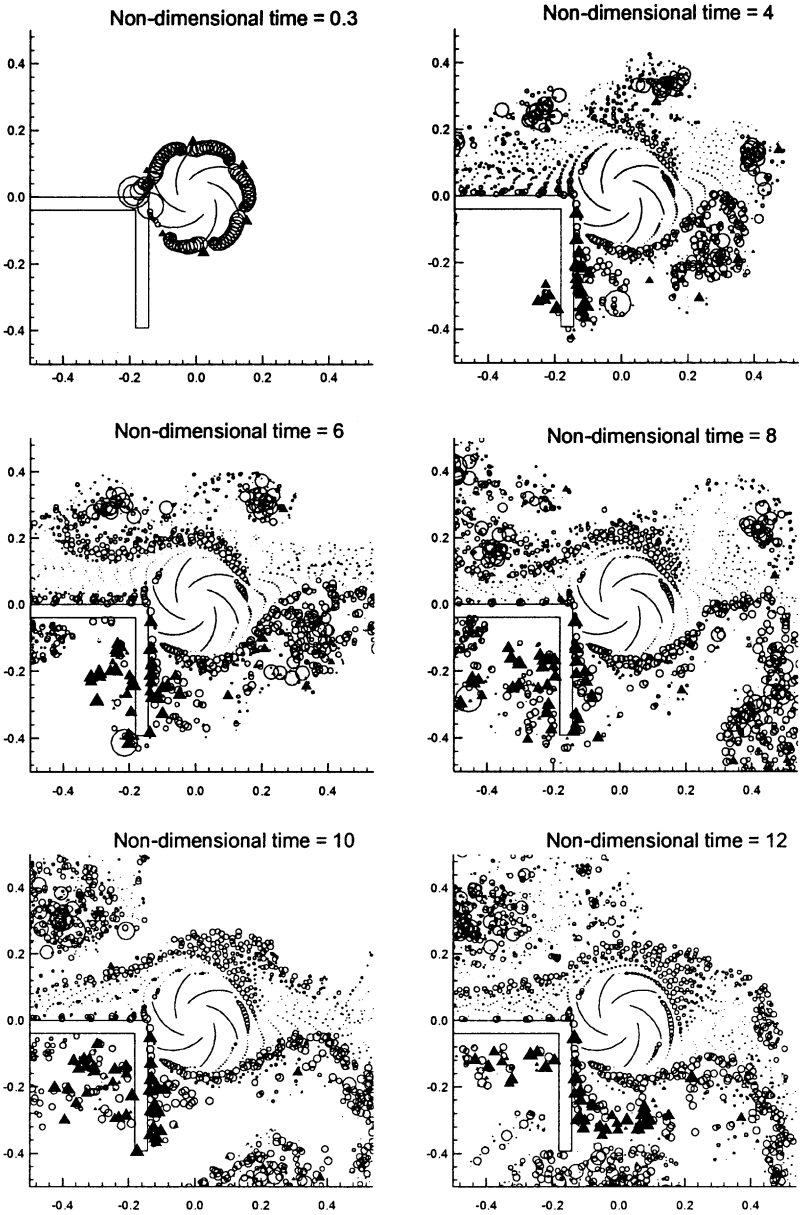

Fig. 9. Distribution of shed vortices with time at 3000 r.p.m.

3. Numerical results

3.1. Validation of the Kirchhoff–Helmholtz BEM

In order to validate the developed Kirchhoff–Helmholtz BEM, it is necessary to compare the numerical results with that of conventional BEM. The first test problem is for a point monopole and dipole sources in the free field. We compare the acoustic field generated from a point monopole and dipole source with the acoustic field from the Kirchhoff surface. The Kirchhoff surface surrounds the point source, and the acoustic value at the mesh point can be obtained. In Fig. 4(a), the acoustic fields by a point monopole and by a Kirchhoff surface are shown. The shape of Kirchhoff surface is a rectangle box, but the shape does not influence the results. The Kirchhoff source surrounds the monopole and the acoustic value of the mesh point obtains from the monopole source. Fig. 4(b) shows the acoustic field generated from a dipole source and Kirchhoff source, which have the information of the dipole source. The comparison shows a good agreement. But, the Kirchhoff surface of 6 elements shows some deviation from the acoustic source. But for 24 elements, the acoustic fields show good agreements.

In order to validate the Kirchhoff–Helmholtz BEM for an interior domain, we calculate the monopole source within the rectangular box as shown in Fig. 5. In Fig. 5(b), we use the Kirchhoff

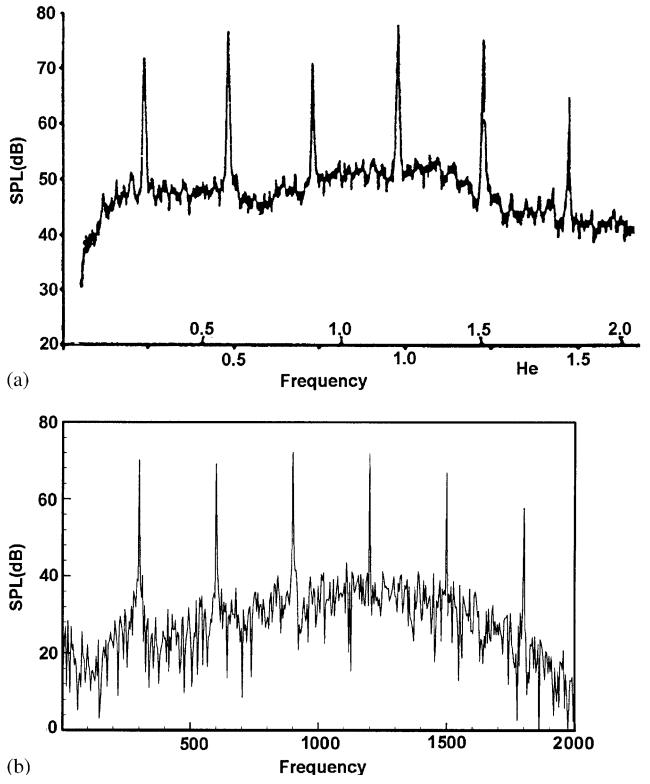

Fig. 10. Comparisons of the frequency spectrum. (a) Measured spectrum [1]. (b) Calculated spectrum (present calculation).

source instead of the monopole point source. The acoustic fields generated by these two different sources are shown in Fig. 6. Both results show good agreements. So, we conclude that the Kirchhoff surface source can replace the conventional acoustic source.

3.2. Flow field calculation

Numerical calculations were conducted for a centrifugal impeller with a rectangle wedge placed close to the impeller tip. This is experimentally tested by Weidemann [1]. The impeller has six blades and rotates at 1200–4100 r.p.m. The inlet diameter and inlet angle of the impeller are 0.112 m and 23.5°; the outlet diameter and outlet angle is 0.28 m and 33.5°. For the flow calculation, 160 elements were used along the wedge and 20 elements for each blade. The time step was taken as $\Delta t = T/60$, where $T = 2\pi/\Omega$ is the period of rotation. The impeller should start from 0 to Ω with the tangent hyperbolic function within one revolution in the calculation.

In the sequel, results are presented for six different values of the speed of rotation Ω. 1200, 1800, 2400, 3000, 3600, 4100 r.p.m. cases. Numerical calculations of the flow field are conducted up to 30 non-dimensional times. One non-dimensional time means one revolution of the impeller.

Calculated head variations are shown in Fig. 7. From the figure, it is known that the variation of head is highly unsteady. But the mean head is almost constant, which is related to the performance. As the rotating velocity of the impeller increases, the mean head and the fluctuating magnitude become large. The acoustic pressure is related to the fluctuating values.

The variation of the shed vortex strength with time at the 3000-r.p.m. case is shown in Fig. 8 for each blade. We can see that each blade has a different value but similar fluctuation pattern.

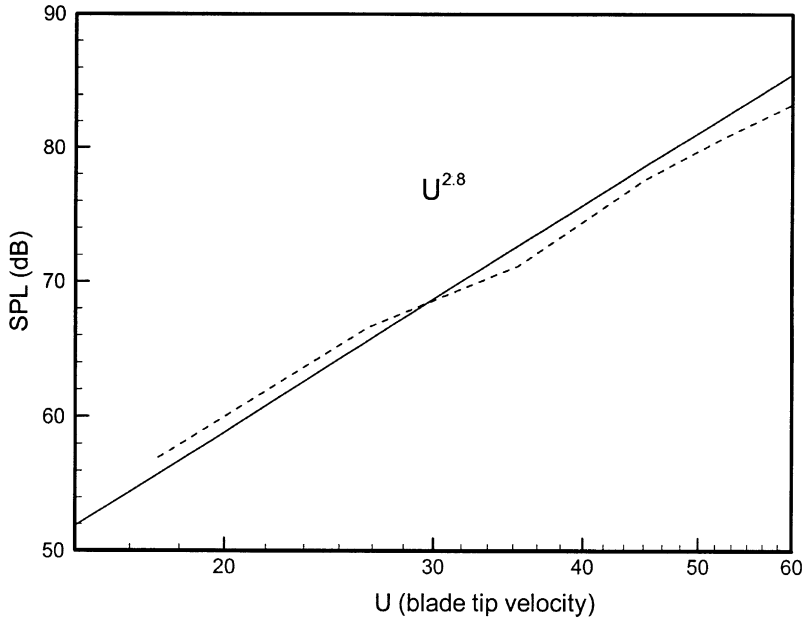

Fig. 11. Determination of the exponent of Mach number (dashed: calculated).

The distributions of shed vortex particles are shown in Fig. 9 for selected times. The circle represents the clockwise rotating vortex particle and the triangle represents the anti-clockwise rotating vortex particle. The size of the symbol indicates the strength of vorticity. The impeller rotates in the anti-clockwise direction. We can find that the direction of shed vortex is changed as the impeller passes the wedge. As the impeller becomes close to the wedge, the shed vortex strength becomes strong. These variations occur periodically and the unsteady fluctuating of the head is due to these periodic interactions.

3.3. Acoustic field calculation—validation of acoustic similarity law

The measured noise spectrum for 3000 r.p.m. is shown in Fig. 10(a) [1]. We can see that the BPF tone and its higher harmonic tones are dominant. The stationary data from 4 to 25 revolutions are used in the calculation of the acoustic pressure. The calculated acoustic pressure is shown in

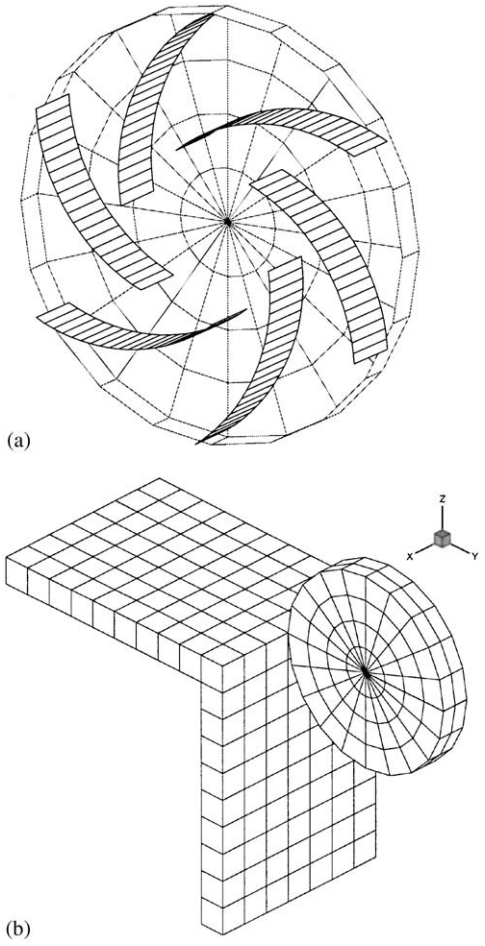

Fig. 12. The mesh of wedge and source grid. (a) Impeller and lower half grid of the Kirchhoff surface. (b) Mesh of the Weidemann's wedge and Kirchhoff surface.

Fig. 10(b). By comparing with the measured data, we can see that the peak frequency and its magnitude are almost the same. The level of broadband noise shows large differences because the prediction method does not consider the effect of the turbulent boundary layer, separated flow, and the inflow turbulence, which mainly generate the broadband noise. They can be approximately calculated if more elegant numerical flow approach such as large eddy simulation (LES) or direct numerical simulation (DNS) for the unsteady flow field calculation is implemented.

The overall sound pressure level is calculated by changing the rotating velocity. The calculated results are shown in Fig. 11. In order to compare with the experiment data, data below the 120 Hz are not considered. The exponent of the impeller tip velocity, v, is obtained as 2.8 from the calculation which is the same value as Weidemann's result [16].

3.4. Acoustic field calculation by BEM

The scattering effect of the wedge is not considered in the previous sections. So the measured and calculated spectrum in Fig. 10 shows some deviations. In order to consider this scattering effect, the Kirchhoff–Helmholtz BEM is introduced. All the time signal data are converted to frequency domain data by FFT. The centrifugal impeller is surrounded by a virtual source grid as shown in Fig. 12(a). At every source grid point, we can calculate the ϕ, and this value is used as source value.

Fig. 13 shows the comparison of the experimental one with the predicted acoustic signal including the scattering effect. In the figure, hollow circles mean the experiment data, rectangle

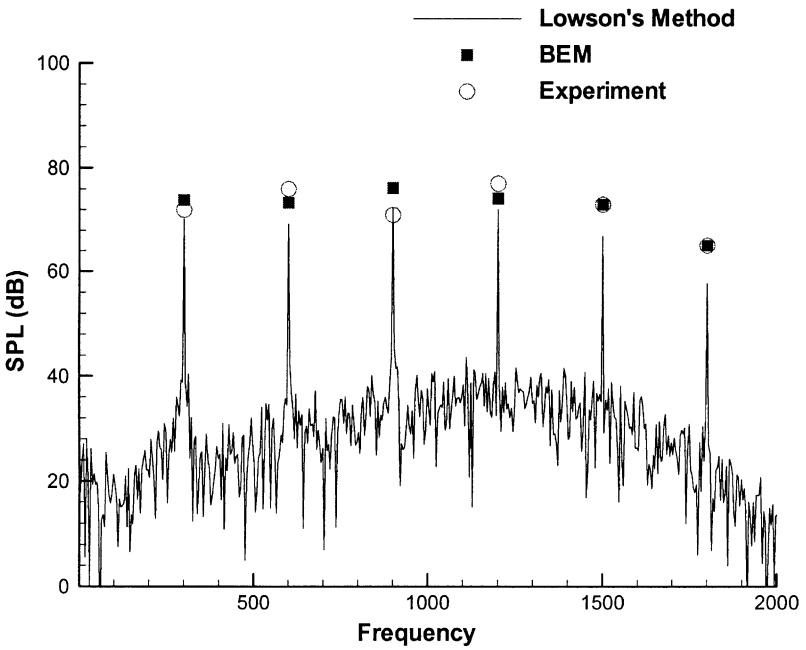

Fig. 13. Comparison of the calculated SPL with Weidemann's measured SPL [1].

means the BEM results and line shows acoustic analogy results—Lowson's results. BEM results show 2–6 dB higher values than the ones obtained from the acoustic analogy. The reflection and scattering effects of the wedge in the BEM make these differences.

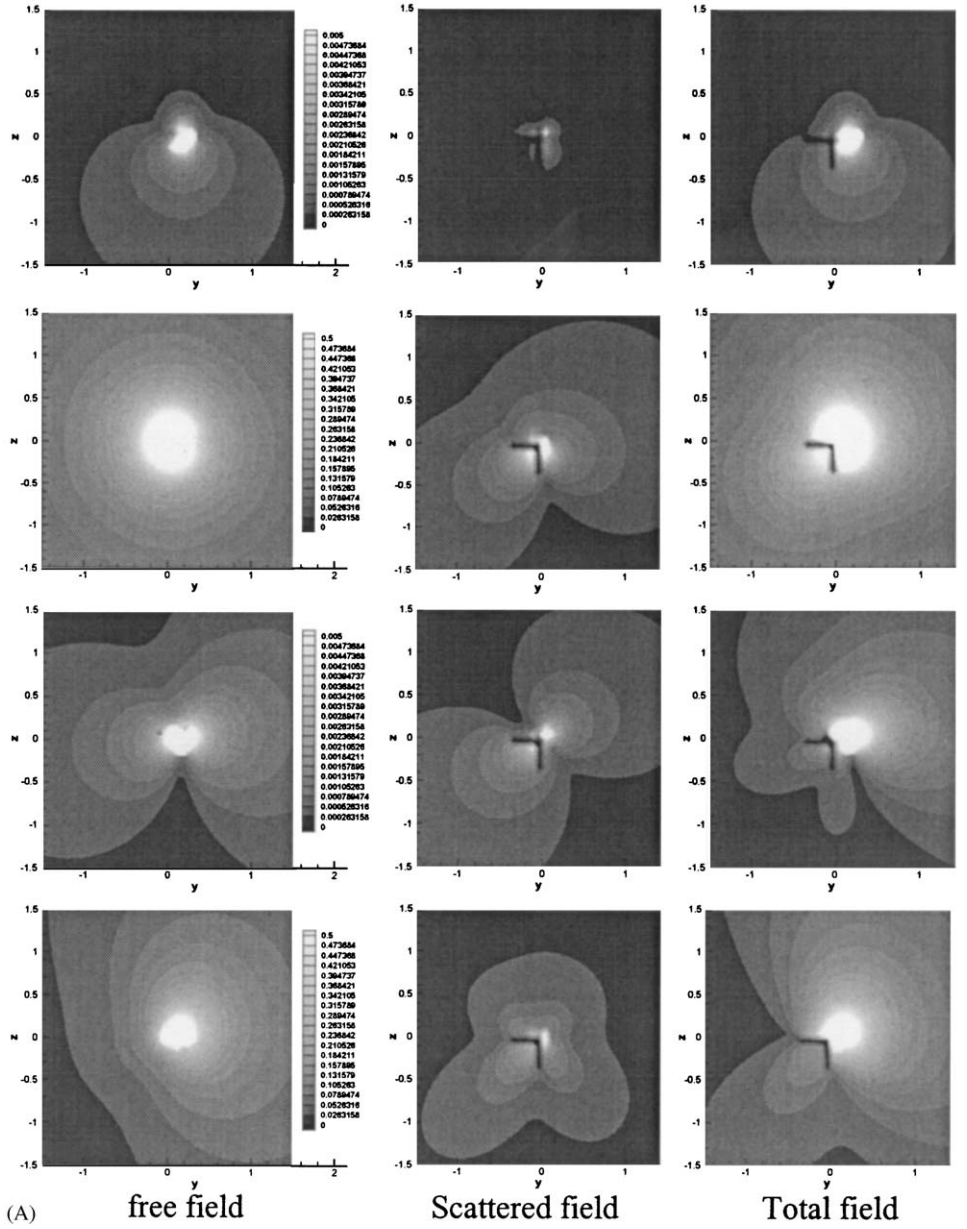

Fig. 14. Calculated acoustic field around the wedge (free, scattering, total acoustic field). (A) From the first row, 150, 300, 450 and 600 Hz.(B) From the first row, 750, 900, 1050 and 1200 Hz. (C) From the first row, 1350, 1500, 1650 and 1800 Hz.

The calculated free field, scattered and total acoustic field are shown in Fig. 14. The left figure shows the freefield results that are generated by impeller. The right figure is the total acoustic field that includes the scattering effects and the free field. In this figure, we can see that the directivity pattern of the acoustic source is similar to the dipole source. The side lobe shows the scattering

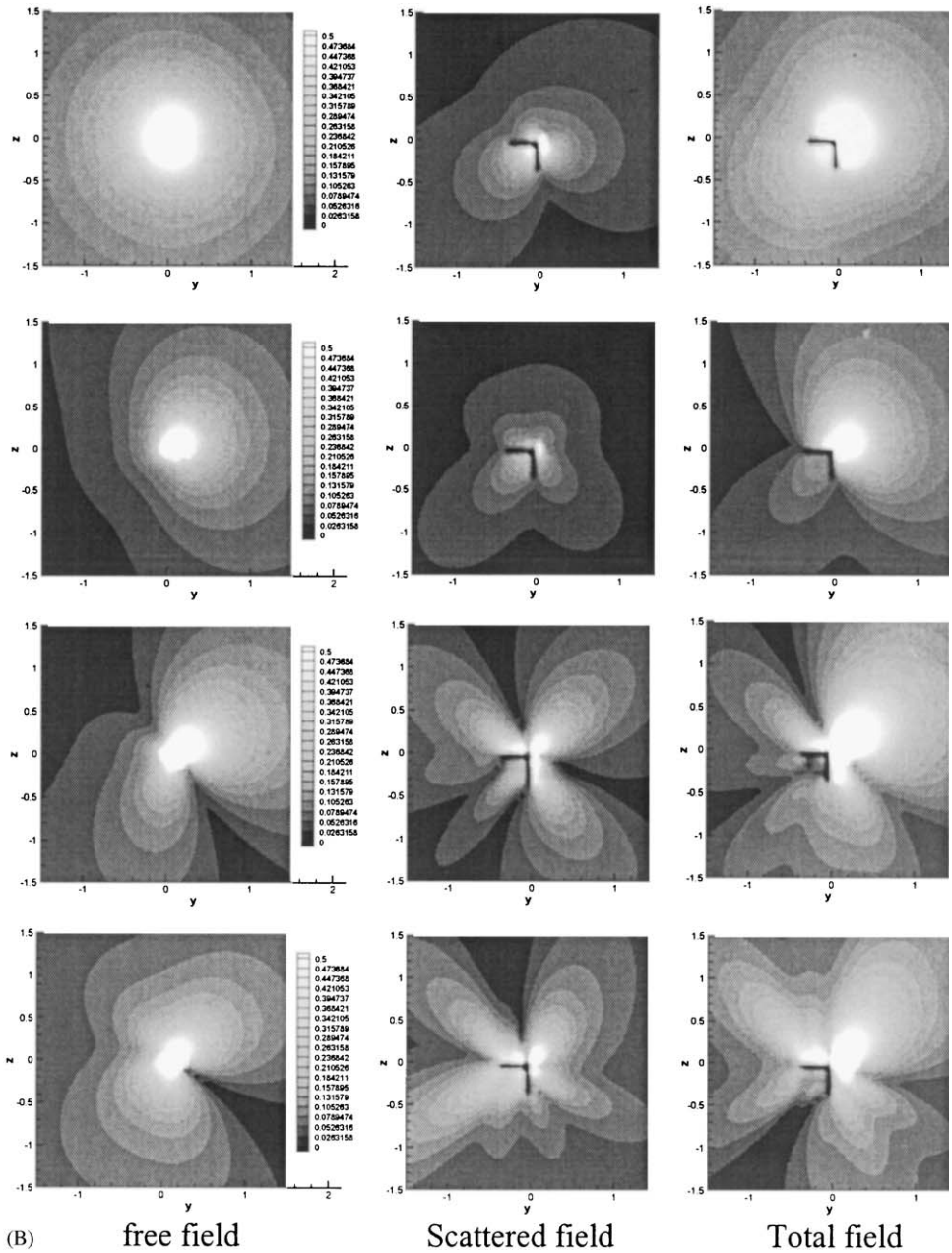

Fig. 14 (*continued*).

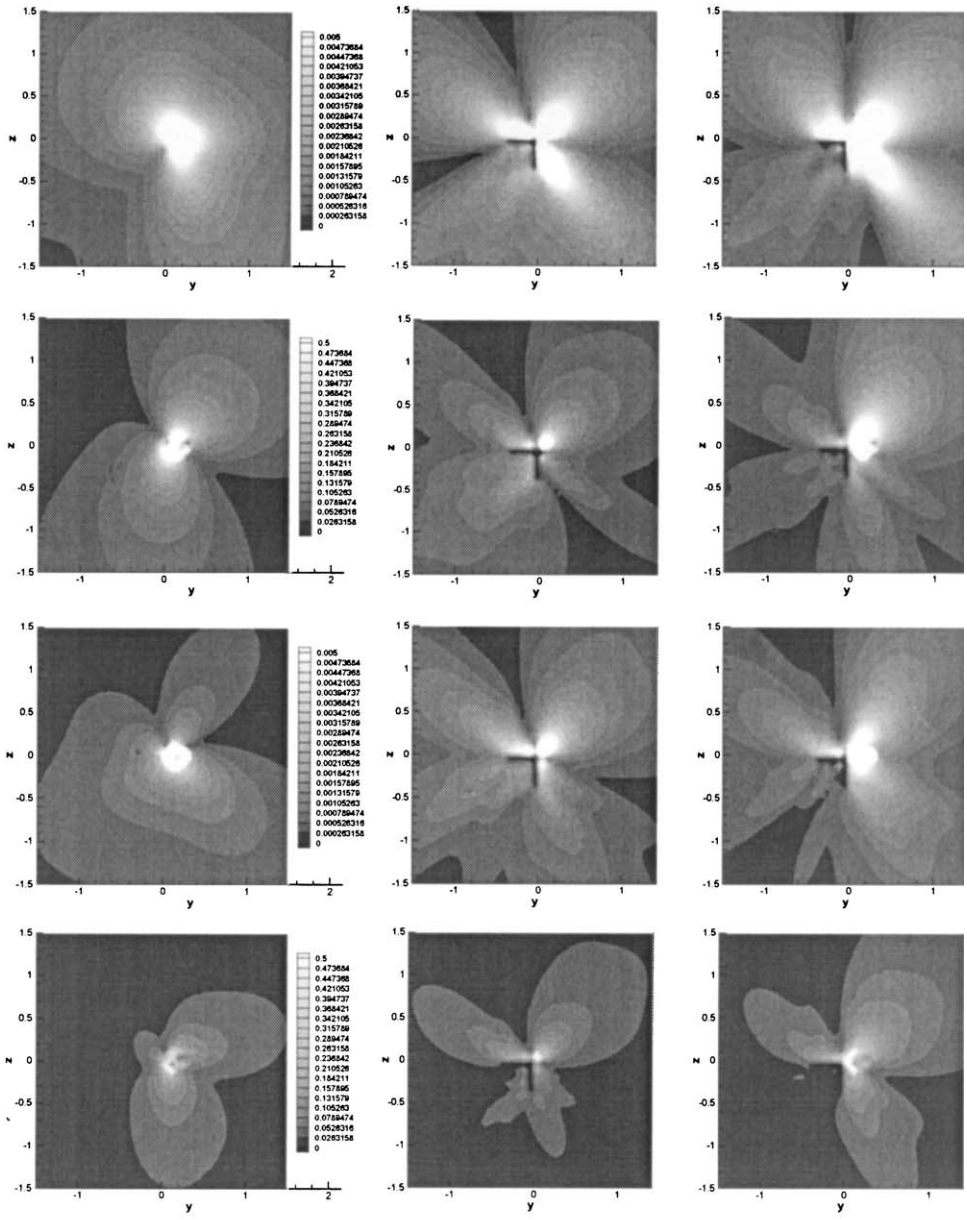

Fig. 14 (*continued*).

and reflection of the source by the wedge. In the low-frequency region, the source acts like a monopole. As the frequency increases, the source acts as a dipole source. The radiation pattern, which is described in Fig. 2, is shown in the results.

From this calculation, we can conclude that the unsteady force fluctuation is generated by the periodic interaction of the impeller blade with the wedge. This force fluctuation is the main source

of acoustic pressure. In order to compare the measured data, the scattering effect should be considered and the newly developed Kirchhoff–Helmholtz BEM is used. The calculated results show good agreements with the experimental ones.

4. Conclusions

The prediction method to identify the noise source generated from a centrifugal fan has been developed. To predict the sound field, unsteady flow fields and unsteady force fluctuations are calculated by the DVM. Unsteady forces associated with the shed vortices at the blade tip are generally due to the interactions between the impeller blades and the wedge.

The numerical results show good agreements with the acoustic similarity law formulated by Weidemann. The predicted impeller tip velocity exponent for the sound pressure is 2.8, which is the same as the experimental one. This means that the numerical method used in this paper can predict the aeroacoustic source of a centrifugal impeller with a good accuracy.

In order to consider the scattering effects of the wedge, the newly developed Kirchhoff–Helmholtz BEM is introduced. These scattering effects are 3–5 dB in this wedge case, compared with the sound field in the calculated free field. Excellent agreements with the experiment data are obtained by using the Kirchhoff–Helmholtz BEM, which included the scattered effects.

References

[1] J. Weidemann, Analysis of the relation between acoustic and aerodynamic parameters for a series of dimensionally similar centrifugal fan rotors, NASA TT F–13, 1971, p. 798.
[2] W. Neise, Noise reduction in centrifugal fans: a literature survey, Journal of Sound and Vibration 45 (1976) 375–403.
[3] T.F. Embleton, Experimental study of noise reduction in centrifugal blowers, Journal of the Aeroacoustical Society of America 35 (1963) 700–705.
[4] W. Neise, G.H. Koopmann, Reduction of centrifugal fan noise by using resonators, Journal of Sound and Vibration 73 (1980) 297–308.
[5] E.E. Morfiadakis, S.G. Voutsinas, D.E. Papantonis, Unsteady flow calculation in a radial flow centrifugal pump with spiral casing, International Journal for Numerical Methods in Fluids 12 (1991) 895–908.
[6] K. Imaichi, Y. Tsujimoto, Y. Yoshida, An analysis of unsteady torque on a two-dimensional radial impeller, Transactions of the ASME 104 (1982) 228–234.
[7] W.H. Jeon, D.J. Lee, An analysis of the flow and sound source of a centrifugal fan, Fifth International Congress on Sound and Vibration 3 (1997) 1333–1340.
[8] M. Kiya, Discrete vortex simulation of separated unsteady flow in a centrifugal impeller, Soviet Union–Japan Symposium on Computational Fluid Dynamics, 1988, pp. 1–7.
[9] R.C. Chanaud, Aerodynamic sound from centrifugal-fan rotors, Journal of the Aeroacoustical Society of America 37 (1965) 969–974.
[10] W. Neise, Application of similarity laws to the blade passage sound of centrifugal fans, Journal of Sound and Vibration 43 (1975) 61–75.
[11] L. Mongeau, D.E. Thompson, D.K. Mclaughlin, Sound generation by rotating stall in centrifugal turbomachines, Journal of Sound and Vibration 163 (1) (1993) 1–30.
[12] W. Neise, Review of fan noise generation mechanisms and control methods, An International INCE Symposium, Senlis, France, 1992, pp. 45–56.

[13] M.V. Lowson, The sound field for singularities in motion, Proceedings of the Royal Society of London, Series A 286 (1965) 559–572.
[14] H.A. Schenck, Improved integral formulation for acoustic radiation problems, Journal of the Acoustical Society of America 44 (1968) 41–58.
[15] A.F. Seybert, B. Soenarko, F.J. Rizzo, D.J. Shippy, An advanced computational method for radiation and scattering of acoustic waves in three dimensions, Journal of the Acoustical Society of America 77 (1985) 362–368.
[16] W.H. Jeon, D.J. Lee, An analysis of the flow and aerodynamic acoustic sources of a centrifugal impeller, Journal of Sound and Vibration 222 (3) (1999) 505–511.